Biogeosciences Discuss., 10, 19731–19772, 2013
www.biogeosciences-discuss.net/10/19731/2013/
doi:10.5194/bgd-10-19731-2013

Biogeosciences Discussions
Open Access

A numerical analysis of the role of the microbial loop in regulating nutrient stoichiometry and phytoplankton dynamics in a eutrophic lake

Y. Li[1,2], G. Gal[3], V. Makler-Pick[4,5], A. M. Waite[6], L. C. Bruce[1,6], and M. R. Hipsey[1,6]

[1]Environmental Dynamics and Ecohydrology, School of Earth and Environment, The University of Western Australia, Crawley WA 6009, Australia
[2]School of Environmental Science and Engineering, Ocean University of China, Qingdao 266100, China
[3]Kinneret Limnological Laboratory, Israel Oceanographic and Limnological Research, Migdal 14950, Israel
[4]Faculty of Civil and Environmental Engineering, Technion-Israel Institute of Technology, Haifa 32000, Israel
[5]Oranim Academic College of Education, Kiryat Tivon 36006, Israel
[6]The Oceans Institute, The University of Western Australia, Crawley WA 6009, Australia

Received: 8 July 2013 – Accepted: 31 July 2013 – Published: 16 December 2013

Correspondence to: M. R. Hipsey (matt.hipsey@uwa.edu.au)

Published by Copernicus Publications on behalf of the European Geosciences Union.

Abstract

The recycling of organic material through bacteria and microzooplankton to higher trophic levels, known as the "microbial loop", is an important process in aquatic ecosystems. Here the significance of the microbial loop in influencing nutrient supply to phytoplankton is investigated in Lake Kinneret (Israel) using a coupled hydrodynamic-ecosystem model. The model was designed to simulate the dynamic cycling of carbon, nitrogen and phosphorus through bacteria, phytoplankton and zooplankton functional groups, with each pool having unique C : N : P dynamics. Three microbial loop submodel configurations were used to isolate mechanisms by which the microbial loop could influence phytoplankton biomass, considering: (i) the role of bacterial mineralization, (ii) bacterial ability to compete for dissolved inorganic nutrients, and (iii) the effect of micrograzer excretion. The nutrient flux pathways between the abiotic pools and biotic groups and the patterns of biomass and nutrient limitation of the different phytoplankton groups were quantified for the different model configurations. Considerable variation in phytoplankton biomass and dissolved organic matter demonstrated the sensitivity of predictions to assumptions about microbial loop operation and the specific mechanisms by which phytoplankton growth was affected. Comparison of the simulations identified that the microbial loop most significantly altered phytoplankton growth by periodically amplifying internal phosphorus limitation due to bacterial competition for phosphate to satisfy their own stoichiometric requirements. Importantly, each configuration led to a unique prediction of the overall community composition, and we conclude that the microbial loop plays an important role in nutrient recycling by regulating not only the quantity, but also the stoichiometry of available N and P that is available to primary producers. The results demonstrate how commonly employed simplifying assumptions about model structure can lead to large uncertainty in phytoplankton community predictions and highlight the need for aquatic ecosystem models to carefully resolve the variable stoichiometry dynamics of microbial interactions.

BGD
10, 19731–19772, 2013

1 Introduction

One of the principal objectives for water quality management of freshwater bodies is to reduce the magnitude and frequency of nuisance algal blooms. Excess nutrients are generally implicated in the production of nuisance blooms since they fuel primary production and organic matter accumulation (Elser, 1999). In trying to understand these processes much work in limnology is based on the classic "N-P-Z-D" (nutrients-phytoplankton-zooplankton-detritus) paradigm, which assumes a relatively simple flow of nutrients to autotrophic and then heterotrophic pools. However, it is now well-documented both in oceanographic and, to a lesser extent, in limnological applications, that higher order predators such as crustacean zooplankton or fish can be supported by two paths: the so-called "green" (algal-based) and "brown" (detrital-based) food web components (Moore et al., 2004). The latter refers to the dynamics of the heterotrophic bacteria and the microzooplankton grazers (defined here as size less than 125 µm to account for rotifers, ciliates, and juvenile macrograzers, Thatcher et al., 1993) – often termed the "microbial loop". This has been shown to play an important role in shaping carbon fluxes in lakes and in enhancing nutrient cycling at the base of food webs, including in Lake Kinneret which is the focus in this study (Stone et al., 1993; Berman et al., 2010; Hart et al., 2000; Hambright et al., 2007).

Less well understood is how the microbial loop can affect patterns of phytoplankton growth and thus potentially shape phytoplankton succession. There are four main mechanisms by which microbial loop processes are thought to influence phytoplankton dynamics: (1) the provision of bacterially mineralized nutrients for phytoplankton growth, (2) the provision of an alternative food source for zooplankton since micrograzers prey on bacteria instead of small phytoplankton; (3) the excretion of readily available nutrients by micrograzers that support primary production (Johannes, 1965; Wang et al., 2009); and (4) the competition of bacteria with phytoplankton for inorganic nutrients when organic detritus becomes nutrient depleted (Barsdate et al., 1974; Bratbak and Thingstad, 1985; Stone, 1990; Kirchman, 1994; Caron, 1994; Joint et al., 2002;

BGD
10, 19731–19772, 2013

Danger et al., 2007). The relative significance of each of these mechanisms, and in particular how they interact in a dynamic environment to shape food web dynamics and influence net productivity, remains unclear.

Models of lake ecosystems are increasingly common to support management and analysis of water quality problems, acting as "virtual" laboratories for exploring ecosystem processes particularly for questions where empirical studies would be difficult to undertake (Van Nes and Scheffer, 2005; Mooij et al., 2010). In most models published to date it is generally assumed that the biomass of heterotrophic bacteria is fairly stable and that the majority of bacterial production is lost to respiration (Cole, 1999). As a result, most quantitative models of carbon and nutrient fluxes in freshwater ecosystems essentially simplify microbial loop processes by assuming a relatively static mineralisation rate of organic material and simulating direct zooplankton consumption of detritus as a proxy for microzooplankton consumption of bacteria (e.g., Janse et al., 1992; Saito et al., 2001; Bruce et al., 2006; Mooij et al., 2010). These simplifications do not capture the range of nutrient "adjustments" that occur during microbial loop processes, since stoichiometric composition of organisms and the fluxes between them are in reality neither uniform nor static (Elser and Urabe, 1999; Sterner and Elser, 2002). Whilst representation of microbial loop processes has been developed in marine ecosystem models (e.g., Faure et al., 2010), there uptake in freshwater ecosystem models has been limited and none to our knowledge simultaneously resolve the microbial loop and the dynamic stoichiometry of carbon (C), nitrogen (N) and phosphorus (P).

As background to this study, there have been several attempts to incorporate the microbial loop into Lake Kinneret ecosystem models. Initially, a steady-state C flux model was developed to examine C cycling through the planktonic biota, including consideration of the microbial loop (Stone et al., 1993; Hart et al., 2000). A one dimensional (1-D) coupled hydrodynamic-ecosystem model (DYRESM-CAEDYM) was presented by Bruce et al. (2006), which focused specifically on the zooplankton dynamics and their contribution to nutrient recycling. However, the model presented by Bruce et al. (2006) had a simplistic representation of the microbial loop dynamics, and did not in-

BGD
10, 19731–19772, 2013

dividually simulate two important cyanobacterial species, (*Microcystis* sp. and *Aphanizonmimen* sp.), that are important to the health of the ecosystem (Zohary, 2004) and sensitive to stoichiometric constraints within the food web. Gal et al. (2009) expanded this model to include a dynamic microbial loop parameterization and accounted for the two cyanobacterial species listed above and validated the model approach against a comprehensive dataset.

This study adapts the previously validated model with the aim of isolating the significance of the microbial loop on the phytoplankton patterns within the lake. Since the microbial loop can regulate both the quantity and stoichiometry of nutrient transfers via organic matter recycling (Li et al., 2013), three different microbial loop model structural configurations were designed and analysed to unravel how the microbial loop processes identified above combine to affect phytoplankton dynamics and stoichiometry of nutrient transfers through the planktonic food web. The results highlight the importance of resolving the variable stoichiometry of microbial interactions in aquatic models.

2 Method

2.1 Site description

Lake Kinneret (Sea of Galilee) is a large monomictic lake located in the Syrian–African Rift Valley in north-eastern Israel. It covers an area of 170 km^2, is 21 km long and 16 km wide, has a maximum depth of 43 m, and has been the focus of considerable limnological research over the past few decades. Major phytoplankton groups present in the lake include *Peridinium* sp., *Aulacoseira* sp., *Aphanizomenon* sp., *Microcystis* sp., and nanophytoplankton. A number of zooplankton species occur in the lake and can be grouped as rotifers, ciliates, and herbivorous (cladocerans and coepodites) and predatory zooplankton (adult copepods). The maximum ciliate abundance is observed in autumn, generally preceding a metazooplankton peak. Heterotrophic nanoflagellates

BGD
10, 19731–19772, 2013

are most abundant in winter and spring, and least abundant in autumn. Bacteria numbers are highest during the decline of the *Peridinium gatunense* (hereafter referred to as *Peridinium*) bloom and are the lowest during the winter (Hadas et al., 1998). Lake Kinneret was once well known for seasonal blooms of *Peridinium* that regularly occurred until the late 1990s (Zohary et al., 1998; Zohary, 2004; Roelke et al., 2007). However, observations over the last decade have seen a major decline in Peridinium and a disruption in the historically stable patterns of phytoplankton succession (Zohary, 2004). In response the biomass of *Aulacoseira* blooms has changed and the contribution of cyanobacteria and nanophytoplankton to the total phytoplankton biomass has increased in summer. Due to reduced water quality, the occurrence of nuisance cyanobacterial blooms is an increasing concern (Ballot et al., 2011).

2.2 Model overview and approach

To examine how the microbial loop can influence patterns of phytoplankton growth, a one dimensional hydrodynamic-ecological model (DYRESM-CAEDYM) was applied to the lake for the period from 1997–2001. The results of alternative microbial loop sub-model configurations were compared to evaluate the relative importance of the four key mechanisms by which the microbial loop can affect phytoplankton dynamics.

2.2.1 General hydrodynamic-ecological modelling approach

DYRESM-CAEDYM has previously been applied to Lake Kinneret to which readers are also referred (Gal et al., 2003, 2009; Bruce et al., 2006; Makler-Pick et al., 2011a, b; Li et al., 2013). The specific configuration adopted here is extended from Gal et al. (2009), with three microbial loop sub-model configurations applied, described below (Fig. 1). The model simulates phytoplankton dynamics, bacterial production, carbon and nutrient recycling, sediment-water interactions, and relevant inflow, outflow and mixing processes. In each simulation conducted, five phytoplankton groups are included, each with three state variables (internal C, N, and P, denoted as *A*, *AIN*, and *AIP*, respec-

BGD
10, 19731–19772, 2013

tively): *Peridinium* (A_1), *Microcystis* (A_2), *Aphanizomenon* (A_3), nanophytoplankton (A_4) and *Aulocaseira* (A_5). Three zooplankton functional groups, Z, each with fixed internal nutrient ratios, were also simulated: predatory copepods (Z_1), macrograzers (Z_2), microzooplankton (Z_3). Bacteria (B) were modeled as a separate state variable for two of the microbial loop configurations. An additional ten nutrient variables (FRP, NO_3, NH_4, DIC, DOC, DON, DOP, POC, PON, POP), and dissolved oxygen (DO) were also modeled, giving a total of 30 biogeochemical state variables (Table 1).

2.2.2 Bacteria and microbial loop sub-models

The three alternative microbial loop sub-model configurations are tested to explore their impacts on the simulation of phytoplankton growth include (Table 2): (1) an assumed constant bacteria biomass state variable using constant organic matter mineralization rates and microzooplankton grazing directly on POM (NOBAC hereafter); (2) bacteria simulated with dynamic biomass and hence mineralization rates, but unable to take up dissolved inorganic N and P (BAC-DIM hereafter); (3) dynamic bacteria (as per 2) with an additional ability for supplementing their internal nutrient requirement with dissolved inorganic N and P (PO_4 and NO_3/NH_4) if the available organic matter becomes nutrient deplete (BAC+DIM hereafter). The general mathematical description of the mass balance for each of the variables and associated notations are in Table 3. For each configuration, parameterization of the common microbial loop process pathways are described in detail next and summarized in Table 4. For other CAEDYM variable descriptions, process equations and parameter values and justifications, readers are referred to Gal et al. (2009).

Common processes in all configurations:

POM hydrolysis: This process considers the enzymatic hydrolysis and decomposition (D_{POM}) of particulate detrital material, limited by dissolved oxygen concentration (DO) and bacterial biomass (B) if bacteria are simulated:

$$D = \mu_{POM\,max} f_B^T(T) \min\left[f_B^{DOB}(DO) f_B(B)\right] POM \quad (1)$$

BGD
10, 19731–19772, 2013

where $\mu_{\mathrm{POM\,max}}$ is the maximum transfer of POM to DOM, and refers to one of $\mu_{\mathrm{POC\,max}}$, μ_{PONmax}, or μ_{POPmax} (Table 4).

DOM mineralization: Whilst the mineralization of DOM to DIM is common to all configurations, when the bacteria state variable is included the process adopts a two-stage breakdown pathway as shown in the subsequent details of BAC-DIM and BAC+DIM configurations. The general rate of DOC breakdown/uptake (U_{DOC}) is simulated as:

$$U_{\mathrm{DOC}} = \begin{cases} \mu_{\mathrm{DOC\,max}} f_B^T(T) f_B^{\mathrm{DOB}}(DO)\mathrm{DOM} & \mathrm{NOBAC} \\ \mu_{\mathrm{DECDOM}} f_B^T(T) \min\left[f_B^{\mathrm{DOB}}(DO) f_B(B)\right]\mathrm{DOM} & \mathrm{BAC\text{-}DIM\ and\ BAC{+}DIM} \end{cases} \quad (2)$$

where μ_{DECDOM} is the maximum bacterial DOM uptake rate, at 20 °C.

Micrograzer grazing: All simulations include microzooplankton (Z_3), which graze either on a lumped detrital pool (NOBAC) or directly on bacteria (BAC-DIM and BAC+DIM). For simplicity, microzooplankton are considered to graze on either bacteria or detritus, since the rate of grazing on small size phytoplankton (A_4) has been reported to be relatively low compared to the rate of bacterial grazing (~ 10 % of total microzooplankton diet in Lake Kinneret: Hambright et al., 2007).

Micrograzer excretion and respiration: In all configurations micrograzers respire (R) and excrete (E) labile organic matter:

$$R_{Z3} = k_{\mathrm{Zr}} f_{Z3}^{T2}(T) Z_3 \quad (3)$$

$$E_{\mathrm{DOC}} = (1 - k_{\mathrm{mf}}) k_{\mathrm{Ze}} G_C(Z_3) \quad (4)$$

where k_{Zr} is the respiration rate and k_{Ze} is the DOC excretion rate. Since micrograzers are configured to have a stable C : N : P requirement, their excretion of N and P is variable in order to balance the other output nutrient fluxes. This is numerically achieved by performing the excretion at the end of the time step after other terms have been

BGD
10, 19731–19772, 2013

accounted for:

$$E_{\mathrm{DON}} = \frac{\mathrm{ZIN}_3^* - Z_3^{t+1} k_{\mathrm{ZIN}_3}}{\Delta t}$$

$$\text{where } \mathrm{ZIN}_3^* = \mathrm{ZIN}_3^t + G_{Z3}(\mathrm{BIN}) - E_{\mathrm{DON}} - M_{Z3} - P_{Z1} \quad (5)$$

$$E_{\mathrm{DOP}} = \frac{\mathrm{ZIP}_3^* - Z_3^{t+1} k_{\mathrm{ZIP}_3}}{\Delta t}$$

$$\text{where } \mathrm{ZIP}_3^* = \mathrm{ZIP}_3^t + G_{Z3}(\mathrm{BIP}) - E_{\mathrm{DOP}} - M_{Z3} - P_{Z1} \quad (6)$$

where k_{ZIN} is the internal ratio of N to C and k_{ZIP} is the internal ratio of P to C of the particular zooplankton class.

Configuration 1 – NOBAC:

This configuration assumes organic matter is mineralized at a rate that is not dependent on the bacterial biomass (i.e., the bacterial biomass is assumed non-limiting and $f_B(B)$ in Eq. (1) is fixed at 1). This approach moves C, N and P fluxes between DOM and DIM proportionally. Since there are no bacteria simulated for micrograzers to graze upon, the grazing preferences were adjusted to consume POM in place of bacteria, thereby assuming bacterial biomass is lumped within the detrital pool. The grazing rate of microzooplankton simplifies to:

$$G_{Z3}(\mathrm{POC}) = g_{\mathrm{MAX}} \frac{\mathrm{POC}}{K_{Z3} + \mathrm{POC}} Z_3 \quad (7)$$

where POC is used to determine the grazing rate and PON and POP are consumed at rate commensurate with their local stoichiometry at the time of grazing. The grazing rate parameter (g_{MAX}) was adjusted to make G_{Z3}(POC) in NOBAC approximately equal to $G_{Z3}(B)$ in BAC+DIM (Table 4), to keep the general C flow and biomass patterns comparable between these simulations.

Configuration 2 – BAC-DIM:

BGD
10, 19731–19772, 2013

This configuration includes the heterotrophic bacteria state variable, B, however, they are restricted to DOM uptake during the mineralization process. Under this scenario, the bacterial biomass and their mineralisation rate increase and decrease depending on temperature and organic matter availability, but their nutrient requirement must be satisfied from the DOM pool. The basic equations for BAC-DIM are similar to NOBAC except the inclusion of the bacterial equation and their associated growth and loss processes (Table 3). Bacterial uptake of DOC is similarly defined using Eq. (2) with $f_B(B)$ defined as:

$$f_B(B) = \frac{B}{K_B + B} \tag{8}$$

Bacterial uptake of DON and DOP is based on the C mineralization rate, converted according to the stoichiometric requirement of N and P (k_{BIN} and k_{BIP}), but limited to the available pool to enforce mass conservation:

$$U_{\mathrm{DON}} = \begin{cases} U_{\mathrm{DOC}} \cdot k_{\mathrm{BIN}} & \mathrm{DON} > U_{\mathrm{DOC}} \cdot k_{\mathrm{BIN}} \Delta t \\ \mathrm{DON} & \mathrm{DON} \leq U_{\mathrm{DOC}} \cdot k_{\mathrm{BIN}} \Delta t \end{cases} \tag{9}$$

$$U_{\mathrm{DOP}} = \begin{cases} U_{\mathrm{DOC}} \cdot k_{\mathrm{BIP}} & DOP > U_{\mathrm{DOC}} \cdot k_{\mathrm{BIP}} \Delta t \\ DOP & DOP \leq U_{\mathrm{DOC}} \cdot k_{\mathrm{BIP}} \Delta t \end{cases} \tag{10}$$

Note that if they cannot support the stoichiometric requirement in line with U_{DOC} from the DON and DOP pool, then they take what is available and UDOC will be reduced accordingly. In this configuration, POM decomposition is also dependent on the changing bacterial biomass through $f_B(B)$ and micrograzers graze on bacteria (B) rather than POM. Therefore $G_{Z3}(B)$ is set as:

$$G_{Z3}(B) = g_{\mathrm{MAX}} \frac{B}{K_{Z3} + B} Z_3 \tag{11}$$

Configuration 3 – BAC+DIM:

BGD
10, 19731–19772, 2013

This configuration is an extension of BAC-DIM where bacteria compete with phytoplankton by supplementing their internal nutrient requirements through the uptake of inorganic nutrients when there is insufficient N and P in the DOM pool to support growth. The bacterial uptake of N and P requires the following additional terms (Table 3):

$$U_{NH_4} = \begin{cases} NH_4 & U_{DOC} \cdot k_{BIN} > (DON + NH_4)\,\Delta t \\ U_{DOC} \cdot k_{BIN} - U_{DON} & U_{DON} < U_{DOC} \cdot k_{BIN}\Delta t \\ 0 & U_{DON} = U_{DOC} \cdot k_{BIN}\Delta t \end{cases} \quad (12)$$

$$U_{NO_3} = \begin{cases} NO_3 & U_{DOC} \cdot k_{BIN} > (DON + NH_4 + NO_3)\,\Delta t \\ U_{DOC} \cdot k_{BIN} - U_{DON} - U_{NH_4} & U_{DON} + U_{NH_4} < U_{DOC} \cdot k_{BIN}\Delta t \\ 0 & U_{DON} + U_{NH_4} \geq U_{DOC} \cdot k_{BIN}\Delta t \end{cases} \quad (13)$$

$$U_{FRP} = \begin{cases} U_{DOC} \cdot k_{BIP} - U_{DOP} & U_{DOP} < U_{DOC} \cdot k_{BIP}\Delta t \\ 0 & U_{DOP} = U_{DOC} \cdot k_{BIP}\Delta t \end{cases} \quad (14)$$

If there is insufficient organic and inorganic N or P to support the carbon uptake rate, U_{DOC}, the growth is limited to enforce mass balance as in configuration 2.

2.3 Analysis procedure

2.3.1 Model sensitivity

Structural sensitivity: The averages of a number of variables from the upper 10 m of the water column were computed over the simulated period (1997–2001) to be consistent with Gal et al. (2009). The physical (T, DO), chemical (TN, TP, NO_3, NH_4, PO_4) and biological variables (A_{1-5}, Z_{1-3}) of the NOBAC, BAC-DIM, and BAC+DIM were statistically compared by One Way ANOVA (5 % significance level, SPSS software version 18.0) and Multiple Comparisons (POST HOC, SPSS software version 18.0) to

BGD
10, 19731–19772, 2013

determine significant differences between the outputs of the alternative microbial loop sub-models.

Parameter sensitivity: In addition, a sensitivity analysis for the impact of the microbial loop parameters on the simulated outputs of the base configuration of BAC+DIM was conducted since this configuration is considered to be the most similar to the actual dynamics of the lake. The limited selection of parameters considered here were chosen based on the detailed analysis of the complete set of ecological parameters by Makler-Pick et al. (2011a), and relevance to the microbial loop processes investigated here. These parameters were scaled individually by +20 % and −20 % according to the procedure in Bruce et al. (2006), to determine the degree of sensitivity of both the state variable concentrations and the major process pathways.

2.3.2 Quantification of pools, fluxes and limitation

To determine the influence of the microbial loop on the food web, the numerous pools and fluxes of C, N, and P were averaged over the simulation period, with both nutrient and biological state variables and fluxes being vertically integrated to provide lake-wide averages.

For each of the phytoplankton groups, the nutrient limitation functions, $f_a(\mathrm{N})$ and $f_a(\mathrm{P})$, at a depth of 1 m below the water surface were assessed to explore the impact of the microbial loop on phytoplankton nutrient limitation. The functions were calculated by the model based on the internal nutrient concentrations (Li et al, 2013):

$$f_a(\mathrm{N}) = \frac{\mathrm{IN}_{\mathrm{MAX}_a}}{\mathrm{IN}_{\mathrm{MAX}_a} - \mathrm{IN}_{\mathrm{MIN}_a}} \left[1 - \frac{\mathrm{IN}_{\mathrm{MIN}_a}}{\mathrm{AIN}_a}\right] \tag{15}$$

$$f_a(\mathrm{P}) = \frac{\mathrm{IP}_{\mathrm{MAX}_a}}{\mathrm{IP}_{\mathrm{MAX}_a} - \mathrm{IP}_{\mathrm{MIN}_a}} \left[1 - \frac{\mathrm{IP}_{\mathrm{MIN}_a}}{\mathrm{AIP}_a}\right] \tag{16}$$

which range from 0 (extreme limitation) to 1 (no limitation).

BGD
10, 19731–19772, 2013

3 Results

3.1 Comparison of model output

The physical, chemical, and biological variables using the explicitly modeled bacteria configuration (BAC+DIM) have been validated in detail by Gal et al. (2009), to which we refer the reader. Here this is compared to the two alternative microbial loop configurations (NOBAC and BAC-DIM). For all configurations, the simulated water level, thermal structure, and dissolved oxygen patterns were almost identical to the earlier version and matched the field data well. The simulated major nutrient results (TN, TP, NO_3, NH_4, and PO_4) for the three configurations were noticeably different in the surface waters, although were similar in the bottom waters where sediment fluxes dominate (Fig. 2a). Most noticeable was the reduced surface water concentrations of NH_4 and NO_3 in the simulated output of BAC-DIM, which also experienced higher PO_4 concentrations. Increased levels of TN were simulated in both the NOBAC and BAC-DIM configurations. All three configurations followed the general seasonal trends, with the most noticeable differences being reduced bacteria and *Peridinium* and increased *Aphanizomenon* concentrations in the BAC-DIM configuration (Fig. 2b); both NOBAC and BAC-DIM simulations had higher error compared with the field data (not shown).

The impact of the three alternative microbial loop configurations on the 15 physical, chemical and biological variables was statistically analyzed by One Way ANOVA and Multiple Comparisons (Table 5). Although the simulated results for T and DO were not significantly different in the three configurations, the simulated results for nutrients were significantly different (p value > 0.05): NH_4, TN, and TP of BAC+DIM were significantly different from BAC-DIM and NOBAC; NO_3 and PO_4 of BAC+DIM were significantly different from BAC-DIM, but similar to NOBAC. Biological variables were also significantly different between these microbial loop configurations: *Peridinium*, *Aphanizomenon*, and microzooplankton of BAC+DIM were significantly different from NOBAC and BAC-DIM; predatory zooplankton within BAC+DIM were significantly different from NOBAC but similar to BAC-DIM; macro-grazers within BAC+DIM and BAC-DIM were

BGD
10, 19731–19772, 2013

significantly different from NOBAC but similar to each other; *Microcystis* of BAC+DIM was also significantly different from BAC-DIM.

3.2 Model parameter sensitivity analysis

Several phytoplankton state variables, microzooplankton and the various process pathways that connected them, were particularly sensitive to a number of key microbial loop parameters (above the 20 % sensitivity level) (Fig. 3). In particular, *Peridinium* and *Microcystis* were sensitive to the diameter of POM particles (d_{POM}) and the bacterial optimum temperature (T_{OPTB}). In addition to d_{POM} and T_{OPTB}, *Microcystis* was sensitive to the zooplankton internal N : C ratio (k_{ZIN}), and *Aphanizomenon* was also highly sensitive to T_{OPTB} (> 50 %). Microzooplankton biomass, bacterial grazing rates and zooplankton excretion rates were strongly sensitive to K_{Ze} (> 30 %), with mild sensitivity to d_{POM}, T_{OPTB}, K_{ZIN}, and the half saturation constant for bacterial function (K_B). The DOM concentration was sensitive to d_{POM}, particularly for N (> 50 %), and the maximum bacterial DOC uptake rate (μ_{DECDOM}), and K_B and k_{ZIN} (> 30 %). Looking specifically at the process pathways, rates of algal excretion and algal uptake were sensitive to $T_{OPTB,}$ particularly in the P cycle (> 30 %). To summarize, the model output was most sensitive to changes in the microbial loop parameters d_{POM}, T_{OPTB}, and K_{Ze}, which had a significant effect on DOM, the biomass of *Peridinium*, cyanobacteria, heterotrophic bacteria, and microzooplankton.

3.3 Nutrient pools

The multi-annual and lake-wide nutrient pools were compared between the three microbial loop configurations to understand how the microbial loop shifts the partitioning of nutrients between different ecosystem compartments (Table 6). In each configuration the stoichiometry of the POM, DOM and DIM pools was free to change, whereas the stoichiometry of zooplankton and bacteria were fixed, and the stoichiometry of phytoplankton was allowed to vary only within the range prescribed by the minimum and

BGD
10, 19731–19772, 2013

maximum parameters of internal nutrient ratios. In each configuration, the DIC pools were similar, but the DOC pool in BAC+DIM was significantly lower (1.79 mg C L^{-1}) than in NOBAC (9.56 mg C L^{-1}) and BAC-DIM (7.81 mg C L^{-1}). Similarly the DON and DOP pools in BAC+DIM were also lower than the corresponding pools in NOBAC and BAC-DIM, even though bacteria were able to take up DIN and DIP to meet their nutrient needs in this configuration. The N : P ratio of DOM in NOBAC was 307 : 1, and with bacteria included (both BAC-DIM and BAC+DIM), the N : P ratios increased significantly to 28 475 : 1 and 3543 : 1 respectively. For configurations with dynamically simulated bacteria, the DIP pools in BAC-DIM (6.4×10^{-3} mg P L^{-1}) and BAC+DIM (5.2×10^{-3} mg P L^{-1}) were higher than that in NOBAC (3.6×10^{-3} mg P L^{-1}), suggesting enhanced P availability for phytoplankton uptake when bacteria were present. The POM pools in BAC-DIM and BAC+DIM were also higher than those in NOBAC.

The biomass of bacteria and zooplankton varied in the different microbial loop configurations, although the N : P stoichiometry of zooplankton and bacteria were fixed at 5 : 1 (bacteria), 27 : 1 (Z_1, predatory zooplankton), 20 : 1 (Z_2, macro-grazers), and 28 : 1 (Z_2, microzooplankton). When bacteria were able to uptake dissolved inorganic nutrients in BAC+DIM, the total bacterial biomass was 2.7 times larger than for BAC-DIM. For zooplankton, biomass of microzooplankton (Z_3) was similar in NOBAC and BAC+DIM and significantly lower in BAC-DIM. For predatory zooplankton (Z_1) simulated biomass was greatest in NOBAC and lowest in BAC+DIM and for macrograzers (Z_2) it was greatest in NOBAC and lowest in BAC-DIM.

The biomass and N : P stoichiometry of the five simulated phytoplankton groups each varied in response to the presence of bacteria in BAC-DIM and then with the addition of bacterial uptake of inorganic nutrients in BAC+DIM. For *Microcystis*, *Peridinium*, nanophytoplankton, *Aulacoseira*, the total C, N, and P content in BAC+DIM were higher than those in BAC-DIM. Similarly, the molar N : P ratios of phytoplankton in BAC+DIM (*Peridinium* 107 : 1; *Microcystis* 8 : 1; nanophytoplankton 47 : 1; *Aulacoseira* 16 : 1) were also higher than their N : P ratios in BAC-DIM (*Peridinium* 59 : 1; *Microcystis* 4 : 1; nanophytoplankton 18 : 1; *Aulacoseira* 10 : 1). Conversely, for *Aphanizomenon*,

BGD
10, 19731–19772, 2013

simulated biomass in BAC-DIM was higher than in BAC+DIM, but no change was observed in their molar N : P ratios (4 : 1). Overall, the total phytoplankton biomass in BAC+DIM was higher than that in BAC-DIM despite this simulation including competition for inorganic nutrients by bacteria.

3.4 Nutrient fluxes

Simulated fluxes of C, N and P from the three microbial loop configurations representing the dominant C, N and P recycling pathways demonstrate significant differences in the relative magnitude of bacterial mineralization, zooplankton excretion, zooplankton grazing, and bacterial competition with phytoplankton for inorganic nutrients (Fig. 4). The simulated rate of algal primary productivity in the BAC+DIM and NOBAC configurations was higher than that simulated in BAC-DIM. Relative to the algal CO_2 fixation rate (defined as 100 % for each simulation), in NOBAC, bacterial respiration returned 32.7 % of the total DIC assimilated by phytoplankton, which was fuelled by DOC from microzooplankton excretion (29.7 %), hydrolysis of particulate detritus (26.7 %) and algal exudation (12.0 %); in BAC-DIM, bacterial respiration returned 43.3 %, fuelled less by DOC from microzooplankton excretion (10.8 %), and more from hydrolysis of particulate detritus (62.8 %) and a similar amount from algal exudation (10.9 %); in BAC+DIM, the magnitude of bacterial respiration was 77.3 % of the total algal fixed carbon, with similar proportions as in BAC-DIM; DOC from microzooplankton excretion (10.2 %), hydrolysis of particulate detritus (69.5 %) and algal exudation (10.7 %).

For N, the algal DIN uptake rates in BAC+DIM and NOBAC were similar, though greater than that in BAC-DIM. The algal DIN uptake percentage in BAC+DIM was 97.0 % relative to the 3.0 % uptake by bacteria (i.e., rates are normalized by the total inorganic N uptake rate). In NOBAC, bacterial mineralization recycled 77.4 % of the total DIN taken up by phytoplankton, with microzooplankton excretion being the primary source of organic N with a similar relative magnitude (68.4 %). In BAC-DIM, bacterial mineralization recycled 47.2 % of N, however only 17.6 % was supplied through microzooplankton excretion due to the lower Z_3 biomass overall. In BAC+DIM, the bacterial

BGD
10, 19731–19772, 2013

mineralization returned 74.3 %, with microzooplankton excretion supplying 21.5 %. As for carbon, in this simulation hydrolysis of particulate detritus was the major source of labile organic nitrogen (> 50 %) relative to that from zooplankton and phytoplankton excretion.

For P, the algal DIP uptake rate in BAC-DIM was higher than in BAC+DIM and NOBAC. In NOBAC, bacterial mineralization replaced 84.2 % of total DIP assimilated by phytoplankton, and zooplankton excretion provided 29.3 % of this P to bacteria, with 41.5 % coming from POM hydrolysis and 10.5 % from algal exudation. In BAC-DIM however, bacterial mineralization recycled 94.0 %, with zooplankton excretion contributing just 12.8 % of this and the remainder coming from POM hydrolysis (67.1 %) and algal exudation (14.1 %). When uptake of DIM by bacteria was simulated (BAC+DIM), DIP uptake shifted significantly to 27.8 % by algae and 72.2 % by bacteria, when normalized relative to the total PO_4 uptake rate. Of this total consumed PO_4, bacterial mineralization was responsible for replacing 95.9 %, and DOM supplied by zooplankton excretion contributed 10.9 %, algal exudation contributed 3.4 % and POM hydrolysis 28.3 %. These fractions were less than that for C an N due to the large rate of supplementation of PO_4.

Note that in all cases the amount of dissolved inorganic N and P that comes from recycling compared to the inflows and sediment fluxes is very high. For example, in BAC+DIM the model predicts that 95.9 % of dissolved inorganic P is sourced from recycling within the water column, only 4.4 % from the sediments, and less from the inflows. For N, the model predicts a reduced dependence on recycling (approximately 67 %), higher sediment flux (22.3 %) and a similar low contribution (0.7 %) from the inflows.

3.5 Patterns of phytoplankton biomass

In conjunction with variability in temperature, light and vertical mixing, changes in nutrient availability resulting from the dynamic nutrient recycling processes leads to variation in phytoplankton nutrient uptake and their nutrient limitation functions, f_a(N) and

BGD
10, 19731–19772, 2013

f_a(P). The different patterns of seasonal variation in the nutrient limitation of the five simulated phytoplankton groups within the three model configurations highlight the potential for microbial loop sub-model structures to influence phytoplankton growth response (Fig. 5). For example, *Peridinium* in NOBAC and BAC+DIM was predicted to have periodic N and P co-limitation, however, in BAC-DIM N limitation was predicted to dominate most of the year. For *Aulacoseira*, in BAC-DIM, N and P co-limitation was experienced most of year, but in NOBAC and BAC+DIM, it displayed more P limitation. For *Microcystis*, in NOBAC, P was the limiting factor for algal growth, however, in BAC-DIM, it was predicted to switch from P limitation to significant N limitation, and in BAC+DIM it experienced significant P limitation with an annual occurrence of N and P co-limitation in spring. For the nanophytoplankton, in NOBAC and BAC+DIM, its growth was P limited with annual N and P co-limitation, but in BAC-DIM the growth switched between N limitation and P limitation annually. For *Aphanizomenon*, in all three configurations, P limitation dominated growth, since it is an N_2-fixing species.

4 Discussion

4.1 Model performance and sensitivity

Given the complexity of interactions affecting phytoplankton succession and bloom dynamics, our ability to accurately predict all species accurately remains a challenge. To date, there are limited modeling examples for a complete lake ecosystem that confidently simulate the successional dynamics of phytoplankton and zooplankton at the level of multiple trophic complexity. This is due to nonlinearity of these complex models and a large number of uncertain parameters and limited validation data (Arhonditsis and Brett, 2004; Rigosi et al., 2010; Mooij et al., 2010). Nonetheless, our models were successful in capturing the seasonal dynamics and the inter-annual variation of the key plankton functional groups in Lake Kinneret, though their absolute concentrations tended to be under predicted. This is not unexpected given we have adopted a later-

BGD
10, 19731–19772, 2013

ally averaged one-dimensional approach which is being compared to inherently patchy field data, known to be particularly relevant during *Peridinium* blooms (e.g., see Ng et al., 2011; Hillmer et al., 2008). However, the models were able to match the annual sequence and timing of the predicted peaks of these blooms, particularly in the BAC+DIM configuration, which we consider to be the closest representation to real lake ecosystem (see Gal et al., 2009 for detailed comparison with field data). Within this simulation the time-scales of growth or decay of the biomass of biological variables generally matched the observed data, and seasonal trends were accurately captured for physical and chemical variables since the model responds significantly to the strong seasonal forcing of the lake (Makler-Pick et al., 2011a). While we acknowledge further improvements could be made, the focus of our study is to use the dynamic model to help us gain insights into the significance of microbial loop processes on phytoplankton growth in accordance with the approach suggested by van Nes and Scheffer (2005) for application of complex models to explore ecological theory. For this purpose, the model captures the variability of key physical, chemical and biological processes to a suitable level to allow us investigate the mechanisms governing the microbial interactions between the configurations.

Accordingly, different microbial loop configurations were found to have a significant impact on the sensitivity of most state variables based on the ANOVA and Multiple Comparison analysis. The predicted surface water nutrient concentrations appeared to be the most sensitive variables to microbial configuration (Fig. 2a and Table 5), with particular sensitivity noted in the concentrations of inorganic nutrients available for phytoplankton growth. Generally, it was noted that in BAC-DIM inorganic nutrients were lower on average even though the total nutrients were higher, due to larger accumulation of organic matter over time indicating that it was not being processed efficiently. In the bottom water, nutrient variables were not sensitive to the microbial loop configurations since the high concentrations of nutrients result from sediment release, and biological activity is limited during the long stratified period due to anoxic conditions.

BGD
10, 19731–19772, 2013

The differences in predicted surface nutrient concentrations between the simulations led to the differences in predicted plankton biomass and growth rates. The structure of the microbial loop model had a significant impact on the total phytoplankton biomass, similar to the results of Faure et al. (2010) for a coastal ecosystem. They demonstrated that DIN and phytoplankton biomass were strongly impacted following explicit inclusion of the microbial loop in their model. In this study, the analysis also includes phosphorus and several different functional groups of phytoplankton and zooplankton, and it was found that nutrients, *Peridinium*, *Aphanizomenon* and zooplankton were the main variables that showed sensitivity to assumptions related to microbial loop configuration.

The parameter sensitivity analysis focused on several bacteria and microbial loop parameters that were hypothesized to have the greatest impact on microbial interactions relevant to the aims of this study, and based on the extensive sensitivity analysis performed by Makler-Pick et al. (2011a). The dominant algal species (*Peridinium*) and the nuisance algal species (*Microcystis*) in the lake were both found to be highly sensitive to two microbial loop parameters: the optimum temperature for bacteria growth (T_{OPTB}) and the diameter of detrital particles (d_{POM}). According to Stoke's law, the diameter of POM particles influences the settling rate of these particles. When the settling velocity is small, the residence time becomes long, so that POM particles persist in the water column for a prolonged period, allowing bacteria to more completely transform and mineralize organic matter. Conversely, higher settling rates increases the loss of TN and TP from the photic zone to the sediment, and identification of d_{POM} as a significant parameter highlights the importance of POM in the nutrient budget and contribution to recycled nutrients. A similar finding was demonstrated by Makler-Pick et al. (2011a) who identified that correct parameterization of d_{POM} was important to ensure a stable balance of TN and TP.

The sensitivity analysis indicated that both microzooplankton biomass and bacterial growth were sensitive to the excretion fraction of the ingested material (K_{Ze}) grazed by microzooplankton. Adjusting this excretion fraction parameter not only impacted their own biomass and grazing rates, but also impacted the biomass of other zooplankton

BGD
10, 19731–19772, 2013

groups and the phytoplankton community more broadly, including *Peridinium*. Although *Peridinium* is not grazed directly by zooplankton, any reduction in nutrient supply from micrograzers leads to reduced P availability and ultimately reduced growth. These results suggest that the interaction between phytoplankton and zooplankton is non linear and that there is a strong potential both for top-down (i.e., grazing-mediated) and bottom-up (i.e., microbial loop nutrient supply) control of phytoplankton. Interestingly, the smaller microzooplankton have a significant overall impact shaping the food web structure in the model simulations despite having the lowest biomass. These findings are in line with the conclusions of Hart et al. (2000) and Hambright et al. (2007), who highlighted the critical role of small micrograzers in the microbial loop processes. Since there exists a range of uncertainty surrounding the parameterization of microzooplankton excretion with large ranges being reported (Fasham et al., 1999; Faure et al., 2010), correct model parameterization remains an important challenge for modellers.

4.2 Role of the microbial loop in regulating nutrient flows

In this study we investigated four mechanisms by which bacterial and microbial loop processes influence phytoplankton via changes in carbon and nutrient cycles: (1) bacterial mineralization of organic nutrients, (2) zooplankton grazing pressure, (3) zooplankton excretion, and (4) bacterial competition with phytoplankton for inorganic nutrients when organic matter quality is poor (i.e., nutrient deplete). By comparing fluxes between pools of C, N and P we were able to gain insights into the role of the microbial loop in the recycling of nutrients.

The complex assemblage of bacteria and zooplankton simulated in the Lake Kinneret model allows us to study the relative affect of microzooplankton grazing and nutrient excretion simultaneously. It is known that microzooplankton can transfer energy and nutrients via bacterial grazing to higher trophic levels due to their small size and high mass-specific grazing rates (Hart et al., 2000; Loladze et al., 2000), and they therefore play an important role in carbon and nutrient recycling (Stone et al., 1993; Dolan 1997; Hambright et al., 2007). In turn, larger zooplankton grazing on microzooplank-

BGD
10, 19731–19772, 2013

ton further provide organic matter for bacterial growth through excretion of nutrient rich organic compounds (DOM) and fecal pellet production (POM) (Peduzzi and Herndl, 1992). From this point of view, the recycling of organic nutrients is facilitated by bacterial consumers rather than bacteria themselves, known as consumer-driven nutrient recycling (CNR) (Elser and Urabe, 1999). The model simulations presented in this study have allowed us to estimate the significance of this pathway and characterize the relative contributions of upward and downward nutrient fluxes of these pathways. For example, in BAC+DIM, as a fraction of algal uptake, microzooplankton excretion was predicted to account for 10 % of C, 22 % of N and 11 % of P returned for mineralization, which was significantly larger than that supplied from algal excretion for N and P (but not for C), and therefore different from the relative proportions consumed through bacterial grazing (18 % for C, 15 % for N and 20 % for P). This highlights the dissimilarity in the C, N and P cycles, and the importance of nutrient adjustments that occur during these microbial interactions.

Bacterial mineralization also had a strong regulatory effect on nutrient recycling, and the model (BAC+DIM) predicted more than 70 % of N and around 95 % of P available for phytoplankton growth was from bacterial mineralization of organic matter. These figures are based on a long-term simulation average and relative contributions were found to vary seasonally in response to temperature and organic matter availability. However, in terms of carbon biomass, the bacterial population was found to be relatively stable. A key result emerging from the simulations is that the lowest concentration of DOC occurred in BAC+DIM, suggesting bacterial metabolism is enhanced when nutrient supplementation is considered. Although bacterial growth is C limited in many lakes (Coveney et al., 1992), bacteria in our simulations were mainly limited by P and also occasionally co-limited by N and P, as indicated by the relative use of inorganic nutrients. In the model, the DOM is assumed to be relatively labile, however in reality different bioavailability of the various organic matter constituents may mean that limitation due to a lack of suitably bioavailable carbon may also occur. There is therefore

BGD
10, 19731–19772, 2013

scope for further extension of the model to understand how processes of mineralization compare when multiple lability fractions of organic matter are considered.

In freshwater ecosystems, the concentration of DON can often be higher than that of DIN, and the DON pool plays an important role in providing N to both bacteria and algae (Berman, 1997, 2001; Berman and Bronk, 2003), though the latter is not considered in our model conceptualization. In the present study, concentrations of DON were higher than those of DIN in NOBAC and BAC-DIM, which fits with observations by Berman and Bronk (2003). However, DON was lower than DIN in BAC+DIM where bacteria biomass and mineralization rates were higher. As a result of increased DIN, DOP became the limiting factor when competition by bacteria for inorganic nutrients was included in the model configuration. Therefore, the variable stoichiometry of organic matter, and different stoichiometric requirements of various process pathways, leads to a complex interplay between the groups (Gaedke et al., 2002) and future studies should further consider the significance of organic matter stoichiometry, microzooplankton excretion rates and rates of nutrient immobilization by bacteria when modeling planktonic food webs (Hessen, 1997; Muller et al., 2001).

4.3 Impact of the microbial loop on the phytoplankton community

Bacterial competition for inorganic nutrients has a two-fold effect on phytoplankton growth by limiting nutrient supply and regulating the N : P ratio of available nutrients. The time series of nutrient limitation functions for the five simulated phytoplankton groups for each of the three alternative microbial loop configurations were used to decipher the effect of bacterial competition on phytoplankton growth. Whilst most freshwaters are considered to be P-limited (Schindler et al., 2008), Elser et al. (2007) discusses that N and P co-limitation is commonly also prevalent. During the simulation period in this study, Lake Kinneret had an average TN : TP ratio $\sim 50:1$ suggesting strong P limitation, as suggested by other authors. However, Gophen (2011) argues N limitation is also occurring, potentially due to large fractions of unavailable organic nitrogen distorting nutrient ratios (Ptanick et al., 2010). The model predictions of the

BGD
10, 19731–19772, 2013

five simulated phytoplankton groups were predominantly P limited, with potential for periodic N and P co-limitation depending on the microbial loop configuration. When organic matter became P depleted, it could not support bacterial growth and therefore PO_4 supplementation of bacteria was evident in the increased uptake rates (Fig. 4c). Bacteria generally have faster P uptake rates relative to phytoplankton (Berman, 1985), which in our model was captured by not limiting the rate of uptake of PO_4 by bacteria; as a result they were able to effectively out-compete the phytoplankton. Several phytoplankton groups experienced differences in the degree of N and P limitation when bacteria were configured not to take up inorganic nutrients (BAC-DIM), as opposed to when bacteria were also consuming inorganic nutrients (BAC+DIM). For *Peridinium* growth, the BAC-DIM simulation was dominated by N limitation, but in BAC+DIM, periods of phosphorus limitation also emerged generally following periods of accelerated growth. For *Aulacoseira*, the lack of bacterial competition for nutrients (BAC-DIM) led to severe N limitation relative to predominant P limitation in BAC+DIM, coinciding with the period of the *Peridinium* bloom. Similarly, for *Microcystis* and the mixed nanophytoplankton community, stronger N limitation simulated in BAC-DIM switched to predominant P limitation in BAC+DIM. The model results indicate that stoichiometric regulation of bacteria through DIM supplementation therfore shifted patterns of phytoplankton nutrient limitation. It therefore follows that bacteria-induced shifts in nutrient limitation can ultimately influence the overall biomass and composition of the phytoplankton community (Andersen et al., 2004). Indeed, here we noted relative differences in the simulated phytoplankton biomass, and in particular, when competition with bacteria for inorganic nutrients was simulated (BAC+DIM), *Peridinium* dominated and *Aulacoseira* also occurred in significant numbers. When this competition is switched off (BAC-DIM), the model simulates reduced *Peridinium* and *Aulacoseira* biomass, with a corresponding significant increase in *Aphanizomenon*. *Microcystis* were also slightly reduced and the nanophytoplankton appeared to exhibit greater seasonality. Interestingly, focusing on the total phytoplankton biomass, the increased competition for nutrients by bacteria somewhat paradoxically led to higher phytoplankton concentrations overall. Therefore

BGD
10, 19731–19772, 2013

the effect of the competition is in shaping the community structure and timing of blooms (see also Li et al., 2013), but overall the micrograzer driven recycling of N and P positively promotes phytoplankton productivity.

The results highlight the importance of understanding the role that the microbial loop plays in nutrient recycling as a critical model component that must be considered when simulating phytoplankton dynamics in freshwater ecosystems. Few lake biogeochemical model studies directly simulate the role of the microbial loop in nutrient recycling (Mooij et al., 2010), with many studies based on extensions of the "N-P-Z-D" approach. In the present study, we identified that the phosphorus content of organic matter is a critical factor driving microbial loop processes, yet this is rarely parameterized in detail within lake ecosystem models, which generally maintain structures equivalent to our NOBAC simulation. We conclude therefore that not only should microbial loop processes and stoichiometric constraints between groups be considered in future model studies but also that the parameterization of these processes be supported with targeted empirical studies.

Acknowledgements. The authors gratefully acknowledge the use of the models DYRESM and CAEDYM (v3.3) developed the Centre for Water Research, University of Western Australia. We also thank the Kinneret Limnological Laboratory (KLL) for making the data available to us. Funding for travel to Lake Kinneret for GLEON12 was provided by the NSF Cyber-enabled and Innovation (CDI) Program, Award #941510. Funding for the PhD study of the first author was from the China Scholarship Council (CSC).

References

Andersen, T., Elser, J., and Hessen, D.: Stoichiometry and population dynamics. Ecol. Lett., 7, 884–900, 2004.

Arhonditsis, G. B. and Brett, M. T.: Evaluation of the current state of mechanistic aquatic biogeochemical modelling, Marine Ecol.-Progress Ser., 271, 13–26, 2004.

BGD
10, 19731–19772, 2013

Ballot, A., Ramm, J., Rundberget, T., Kaplan-Levy, R. N., Hadas, O., Sukenik, A., and Wiedner, C.: Occurrence of non-cylindrospermopsin-producing *Aphanizomenon ovalisporum* and *Anabaena bergii* in Lake Kinneret (Israel), J. Plankton Res., 33, 1736–1746, 2011.

Barsdate, R. J., Prentki, R. T., and Fenchel, T.: Phosphorus cycle of model ecosystems: significance for decomposer food chains and effect of bacterial grazers, Oikos, 25, 239–251, 1974.

Berman, T.: Uptake of (32P)orthophosphate by algae and bacteria in Lake Kinneret, J. Plankton Res., 7, 71–84, 1985.

Berman, T.: Dissolved organic nitrogen utilization by an *Alphanizomenon* bloom in Lake Kinneret, J. Plankton Res., 19, 577–586, 1997.

Berman, T.: The role of DON and the effect of N : P ratios on occurrence of cyanobacterial blooms: implications from the outgrowth of *Aphanizomenon* in Lake Kinneret, Limnol. Oceanogr., 46, 443–447, 2001.

Berman, T. and Bronk, D. A.: Dissolved organic nitrogen: a dynamic participant in aquatic ecosystems, Aq. Microb. Ecol., 31, 279–305, 2003.

Berman, T., Parparov, A., and Yacobi, Y. Z.: Planktonic community production and respiration and the impact of bacteria on carbon cycling in the photic zone of Lake Kinneret, Aq. Microb. Ecol., 34, 43–55, 2004.

Berman, T., Yacobi, Y. Z., Parparov, A., and Gal, G.: Estimation of long-term bacterial respiration and growth efficiency in Lake Kinneret, FEMS Microbiol. Ecol., 71, 351–363, 2010.

Bratbak, G. and Thingstad, T. F.: Phytoplankton-bacteria interactions-an apparent paradox-analysis of a model system with both competition and commensalism, Marine Ecology-Progress Series, 25, 23–30, 1985.

Bruce, L. C., Hamilton, D. P., Imberger, J., Gal, G., Gophen, M., Zohary, T., and Hambright, D.: A numerical simulation of the role of zooplankton in C, N and P cycling in Lake Kinneret, Israel, Ecol. Model., 193, 412–436, 2006.

Burger, D. F., Hamilton, D. P., and Pilditch, C. A.: Modelling the relative importance of internal and external nutrient loads on water column nutrient concentrations and phytoplankton biomass in a shallow polymictic lake, Ecol. Model., 211, 411–423, 2007.

Caron, D. A.: Inorganic nutrients, bacteria, and the microbial loop, Microbial ecology, 28, 295–298, 1994.

Cole, J. J.: Aquatic microbiology for ecosystem scientists: new and recycled paradigms in ecological microbiology, Ecosystems, 2, 215–225, 1999.

BGD
10, 19731–19772, 2013

Coveney, M. F. and Wetzel, R. G.: Effects of nutrients on specific growth rate of Bacterioplankton in oligotrophic lake water cultures, Appl. Environ. Microbiol., 58, 150–156, 1992.
Danger, M., Oumarou, C., Benest, D., and Lacroix, G.: Bacteria can control stoichiometry and nutrient limitation of phytoplankton, Funct. Ecol., 21, 202–210, 2007.
Dolan, J. R.: Phosphorus and ammonia excretion by planktonic protists, Mar. Geol., 139, 109–122, 1997.
Elser J. J.: The pathway to noxious cyanobacterial blooms in lakes: the food web as the final turn, Freshwater Biol., 42, 537–543, 1999.
Elser, J. J. and Urabe J.: The stoichiometry of consumer-driven nutrient recycling: theory, observations, and consiquences, Ecology, 80, 735–751, 1999.
Elser, J. J. Bracken, M. E. S., Cleland, C. S., Gruner, G. S., Harpole, W. S., Hillebrand, H., Ngai, J. T., Seabloom, E. W., Shurin, J. B., and Smith, J. E.: Global analysis of nitrogen and phosphorus limitation of primary producers in freshwater, marine and terrestrial ecosystems, Ecol. Lett., 10, 1135–1142, 2007.
Faure, V., Pinazo, C., Torréton, J. P.,and Jacquet, S.: Modelling the spatial and temporal variability of the SW lagoon of New Caledonia I: a new biogeochemical model based on microbial loop recycling, Mar. Pollut. Bull., 61, 465–479, 2010.
Fasham, M. J. R., Boyd, P. W., and Savidge, G.: Modeling the relative contributions of autotrophs and heterotrophs to carbon flow at a Lagrangian JGOFS station in the Northeast Atlantic: the importance of DOC, Limnol. Oceanogr., 44, 80–94, 1999.
Gaedke, U., Hochstadter, S., and Straile, D.: Interplay between energy limitation and nutritional deficiency: empirical data and food web models, Ecol. Monogr., 72, 251–270, 2002.
Gal, G., Imberger, J., Zohary, T., Antenucci, J. P., Anis, A., and Rosenberg, T.: Simulating the thermal dynamics of Lake Kinneret, Ecol. Model., 162, 69–86, 2003.
Gal, G., Hipsey, M. R., Parparov, A., Wagner, U., Makler, V., and Zohary, T.: Implementation of ecological modeling as an effective management and investigation tool: Lake Kinneret as a case study, Ecol. Model., 220, 1697–1718, 2009.
Gophen, M.: The cladoceran trophic status in the nitrogen limited ecosystem of Lake Kinneret (Israel), J. Environ. Biol., 32, 455–462, 2011.
Gophen, M. and Azoulay, B.: The trophic status of zooplankton communities in Lake Kinneret (Israel), Verhandlungen des Internationalen Verein Limnologie, 28, 836–839, 2002.
Hadas, O. and Berman, T.: Seasonal abundance and vertical distribution of Protozoa (flagellates, ciliates) and bacteria in Lake Kinneret, Israel, Aq. Microb. Ecol., 14, 161–170, 1998.

BGD
10, 19731–19772, 2013

Hambright, K. D., Zohary T., and Gude, H.: Microzooplankton dominate carbon flow and nutrient cycling in a warm subtropical freshwater lake, Limnol. Oceanogr., 52, 1018–1025, 2007.
Hambright, K. D., Zohary, T., Eckert, W., Eckert, S., Schwartz, S. S., Schelske, C. L., Laird, K., and Leavitt, P. R.: Exploitation and destabilization of a warm, freshwater ecosystem through engineered hydrological change, Ecol. Appl., 18, 1591–1603, 2008.
Hart, D. R., Stone, L., and Berman, T.: Seasonal dynamics of the Lake Kinneret food web: the importance of the microbial loop, Limnol. Oceanogr., 45, 350–361, 2000.
Hessen, D.: Stoichiometry in food webs – Lotka revisited, Oikos, 79, 195–200, 1997.
Hillmer, I., van Reenen, P., Imberger, J., and Zohary, T.: Phytoplankton patchiness and their role in the modelled productivity of a large, seasonally stratified lake, Ecol. Model., 218, 49–59, 2008.
Janse, J. H., Aldenberg, T., and Kramer, P. R. G.: A mathematical model of the phosphorus cycle in Lake Loosdrecht and simulation of additional measures, Hydrobiologia, 233, 119–136, 1992.
Johannes, R. E.: Influence of marine protozoa on nutrient regeneration, Limnol. Oceanogr., 10, 434–442, 1965.
Joint, I., Henriksen, P., Fonnes, G. A., Bourne, D., Thingstad, T. F., and Riemann, B.: Competition for inorganic nutrients between phytoplankton and bacterioplankton in nutrient manipulated mesocosms, Aq. Microb. Ecol., 29, 145–159, 2002.
Jorgensen, S. E. and Bendoricchio, G.: Fundamentals of Ecological Modeling, 3rd Edn., Elsevier, 2001.
Kirchman, D. L.: The uptake of inorganic nutrients by heterotrophic bacteria, Microbial Ecology, 28, 255–271, 1994.
Li, Y., Waite, A. M., Gal, G., and Hipsey, M. R.: An analysis of the relationship between phytoplankton internal stoichiometry and water column N : P ratios in a dynamic lake environment, Ecol. Model., 252, 196–213, 2013.
Loladze, I., Kuang, Y., and Elser, J.: Stoichiometry in producer-grazer systems: linking energy flow with element cycling, Bull. Math. Biol., 62, 1137–1162, 2000.
Makler-Pick, V., Gal, G., Gorfine, M., Hipsey, M. R., and Carmel, Y.: Sensitivity analysis for complex ecological models – a new approach, Environ. Modell. Softw., 26, 124–134, 2011a.
Makler-Pick, V., Gal, G., Shapiro, J., and Hipsey. M. R.: Exploring the role of fish in a lake ecosystem (Lake Kinneret, Israel) by coupling an individual-based fish population model to a dynamic ecosystem model, Can. J. Fish. Aq. Sci., 68, 1265–1284, 2011b.

BGD
10, 19731–19772, 2013

Martin-Creuzburg, D., Bec, A., von Elert, E.: Trophic upgrading of picocyanobacterial carbon by ciliates for nutrition of Daphnia magna, Aq. Microb. Ecol., 41, 271–280, 2005.
Mooij, W. M., Trolle, D., Jeppesen, E., Arhonditsis, G., Belolipetsky, P., Chitamwebwa, D. B. R., Degermendzhy, A. G., DeAngelis, D. L., Senerpont Domis de, L. N., Downing, A. S., Elliott, J. A., Fragoso Jr., C. R., Gaedke, U., Genova, S. N., Gulati, R. D., Håkanson, L., Hamilton, D. P., Hipsey, M. R., Hoen, P. J., Hülsmann, S., Los, F. J., Makler-Pick, V., Petzoldt, T., Prokopkin, I., Rinke, K., Schep, S. A., Tominaga, K., Dam Van, A. A., Nes van, E. H., Wells, S. A., and Janse, J. H.: Challenges and opportunities for integrating lake ecosystem modelling approaches, Aq. Ecol., 44, 633–667, 2010.
Moore, J. C., Berlow, E. L., Coleman, D. C., Ruiter, P. C., Dong, Q., Hastings, A., Johnson, N. C., McCann, K. S., Melville, K., Morin, P. J., Nadelhoffer, K., Rosemond, A. D., Post, D. M., Sabo, J. L., Scow, K. M., Vanni, M. J., and Wall, D. H.: Detritus, trophic dynamics and biodiversity, Ecol. Lett., 7, 584–600, 2004.
Muller, E., Nisbet, R., Koojman, S, Elser, J., and McCauley, E.: Stoichiometric food quality and herbivore dynamics, Ecol. Lett., 4, 519–529, 2001.
Ng, S., Antenucci, J. P., Hipsey, M. R., Tibor, G., and Zohary, T.: Physical controls on the spatial evolution of a dinoflagellate bloom in a large lake, Limnol. Oceanogr., 56, 2265–2281, 2011.
Peduzzi, P. and Herndl, G. J.: Zooplankton activity fueling the microbial loop: differential growth response of bacteria from oligotrophic and eutrophic waters, Limnol. Oceanogr., 37, 1087–1092, 1992.
Ptacnik, R., Andersen, T., and Tamminen, T.: Performance of the Redfield ratio and a family of nutrient limitation indicators as thresholds for phytoplankton N vs. P limitation, Ecosystems, 13, 1201–1214, 2010.
Rigosi, A., Fleenor, W., and Rueda, F.: State-of-the-art and recent progress in phytoplankton succession modelling, Environ. Rev., 18, 423–440, 2010.
Roelke, D. L., Zohary, T., Hambright, D. K., and Montoya, J. V.: Alternative states in the phytoplankton of Lake Kinneret, Israel (Sea of Galilee), Freshwater Biol., 52, 399–411, 2007.
Saito, L., Johnson, B. M., Bartholow, J., and Hanna, R. B.: Assessing ecosystem effects of reservoir operations using food web-energy transfer and water quality models, Ecosystems, 4, 105–125, 2001.
Sterner, R. W. and Elser, J. J.: Ecological Stoichiometry, Princeton University Press, New Jersey, 2002.

BGD
10, 19731–19772, 2013

Stemberger, R. S. and Gilbert, J. J.: Body size, food concentration, and population growth in planktonic rotifers, Ecology, 66, 1151–1159, 1985.
Stone, L.: Phytoplankton–bacteria–protozoa interactions – a qualitative model portraying indirect effects, Marine Ecol.-Progress Ser., 64, 137–145, 1990.
Stone, L., Berman, T., Bonner, R., Barry, S., and Weeks, S. W.: Lake Kinneret: a seasonal model for carbon flux through the planktonic biota, Limnol. Oceanogr., 38, 1680–1695, 1993.
Thatcher, S. J., Davis, C. C., and Gardner, G. A.: Physical and chemical effects of macrograzers and micrograzers on enclosed, in situ phytoplankton in a Newfoundland lake, Hydrobiologia, 250, 127–141, 1993.
Thingstad, T. F., Bellerby, R. G. J., Bratbak, G., Børsheim, K. Y., Egge, J. K., Heldal, M., Larsen, A., Neil, C., Nejstgaard, J., Norland, S., Sandaa, R. A., Skjoldal, E. F., Tanaka, T., Thyrhaug, R., and Töpper, B.: Counterintuitive carbon-to-nutrient coupling in an Arctic pelagic ecosystem, Nature, 455, 387–390, 2008.
Van Nes, E. H. and Scheffer, M.: A strategy to improve the contribution of complex simulation models to ecological theory, Ecol. Model., 185, 153–164, 2005.
Wang, H., Jiang, L., and Weitz, J. S.: Bacterivorous grazers facilitate organicmatter decomposition: a stoichiometric modeling approach, FEMS Microbiol. Ecol., 69, 170–179, 2009.
Zohary, T., Pollingher, U., Hadas, O., and Hambright, K. D.: Bloom dynamics and sedimentation of Peridinium gatunense in Lake Kinneret, Limnol. Oceanogr., 43, 175–186, 1998.
Zohary, T.: Changes to the phytoplankton assemblage of Lake Kinneret after decades of a predictable, repetitive pattern, Freshwater Biol., 49, 1355–1371, 2004.

BGD
10, 19731–19772, 2013

Table 1. Overview of the simulated variables configured with DYRESM-CAEDYM.

Notation	CAEDYM Name	Description	Units
Biogeochemical variables			
DOC	DOCL	Dissolved organic carbon concentration	mg C L^{-1}
POC	POCL	Detrital particulate organic carbon concentration	mg C L^{-1}
TN		Total nitrogen concentration	mg N L^{-1}
PON	PONL	Detrital particulate organic nitrogen concentration	mg N L^{-1}
DON	DONL	Dissolved organic nitrogen concentration	mg N L^{-1}
NH4	NH4	Ammonium concentration	mg N L^{-1}
NO3	NO3	Nitrate concentration	mg N L^{-1}
TP		Total phosphorus concentration	mg P L^{-1}
POP	POPL	Detrital particulate organic phosphorus concentration	mg P L^{-1}
DOP	DOPL	Dissolved organic phosphorus concentration	mg P L^{-1}
FRP	PO4	Filterable reactive phosphorus	mg P L^{-1}
DO	DO	Dissolved oxygen concentration	mg O L^{-1}
Biological variables			
N_A		Number of algal groups being simulated (= 5)	–
A		Algal group index (1 . . . N_A)	–
A_1	DINOF	Algae #1 (Dinoflagellate: *Peridinium gatunense* the main, bloom-forming species) C biomass concentration	mg C L^{-1}
A_2	CYANO	Algae #2 (Cyanobacteria: Non N_2 fixing group represented by *Microcystis*, toxin-producing species) C biomass concentration	mg C L^{-1}
A_3	NODUL	Algae #3 (Cyanobacteria: Filamentous N_2 fixing group represented mostly by *Aphanizomenon ovalisporum* and *Cylindrospermopsis cuspis*) C biomass concentration	mg C L^{-1}
A_4	CHLOR	Algae #4 (Nanophytoplankton: A large suite of species that are nanoplanktonic in size and are readily grazed by zooplankton) C biomass concentration	mg C L^{-1}
A_5	FDIAT	Algae #5 (Diatom: *Aulacoseira granulata*, a winter bloom forming filamentous diatom) C biomass concentration	mg C L^{-1}
AIN_1	IN_DIN	Algae #1 (Dinoflagellate: *Peridinium*) internal N concentration	mg N L^{-1}
AIN_2	IN_CYA	Algae #2 (Cyanobacteria: *Microcystis*) internal N concentration	mg N L^{-1}
AIN_3	IN_NOD	Algae #3 (Cyanobacteria: *Aphanizomenon*) internal N concentration	mg N L^{-1}
AIN_4	IN_CHL	Algae #4 (Nanophytoplankton) internal N concentration	mg N L^{-1}
AIN_5	IN_FDI	Algae #5 (Diatom: *Aulacoseira*) internal N concentration	mg N L^{-1}
AIP_1	IP_DIN	Algae #1 (Dinoflagellate: *Peridinium*) internal P concentration	mg P L^{-1}
AIP_2	IP_CYA	Algae #2 (Cyanobacteria: *Microcystis*) internal P concentration	mg P L^{-1}
AIP_3	IP_NOD	Algae #3 (Cyanobacteria: *Aphanizomenon*) internal P concentration	mg P L^{-1}
AIP_4	IP_CHL	Algae #4 (Nanophytoplankton) internal P concentration	mg P L^{-1}
AIP_5	IP_FDI	Algae #5 (Diatom: *Aulacoseira*) internal P concentration	mg P L^{-1}
N_Z		Number of zooplankton groups being simulated (= 3)	–
Z		Zooplankton group index (1 . . . N_Z)	–
Z_1	ZOOP1	Zooplankton #1 (Predators: adult copepods, predatory rotifers) C biomass concentration	mg C L^{-1}
Z_2	ZOOP2	Zooplankton #2 (Large herbivores/macrozooplankton: cladocerans, copepodites) C biomass concentration	mg C L^{-1}
Z_3	ZOOP3	Zooplankton #3 (Microzooplankton: copepod nauplii, most rotifers, ciliates, heterotrophic flagellates) C biomass concentration	mg C L^{-1}
ZIN_1		Zooplankton #1 (Predators: *Copepods*) internal N concentration	mg N L^{-1}
ZIN_2		Zooplankton #2 (Macro-grazers: *Cladocerans*) internal N concentration	mg N L^{-1}
ZIN_3		Zooplankton #3 (Micro-grazers: *Rotifers/Ciliates*) internal N concentration	mg N L^{-1}
ZIP_1		Zooplankton #1 (Predators: *Copepods*) internal P concentration	mg P L^{-1}
ZIP_2		Zooplankton #2 (Macro-grazers: *Cladocerans*) internal P concentration	mg P L^{-1}
ZIP_3		Zooplankton #3 (Micro-grazers: *Rotifers/Ciliates*) internal P concentration	mg P L^{-1}
B	BAC	Heterotrophic bacterial C biomass concentration	mg C L^{-1}
BIN		Heterotrophic bacterial internal nitrogen concentration	mg N L^{-1}
BIP		Heterotrophic bacterial internal phosphorus concentration	mg P L^{-1}

BGD
10, 19731–19772, 2013

Table 2. Summary of three microbial loop simulations configured.

Model description	NOBAC	BAC-DIM	BAC+DIM
Phytoplankton: Zooplankton: Bacteria:	A_{1-5} Z_{1-3} 0	A_{1-5} Z_{1-3} 1	A_{1-5} Z_{1-3} 1
Microzooplankton grazing	Assumes bacteria combined in detritus pool, which is grazed by microzooplankton	Assumes a dynamic heterotrophic bacterial pool that is grazed upon by microzooplankton, including C, N and P transfer	Assumes a dynamic heterotrophic bacterial pool that is grazed upon by microzooplankton, including C, N and P transfer
Organic matter breakdown	Occurs at a constant rate, and C, N and P are broken down in a constant proportion	DOM consumption linked to bacterial biomass. Rate of mineralization and bacterial biomass growth slows if bacteria can not satisfy N or P requirement from the DOM pool.	DOM consumption linked to bacterial biomass. Rate of mineralization not linked to DOM stoichiometry and bacteria consume NO_3 or PO_4 if they cannot satisfy N or P requirement from the DOM pool.
Mechanisms by which microbial loop impacts phytoplankton	(i) bacterial mineralization of nutrients	(i) bacterial mineralization of nutrients (ii) micrograzers respond to variable bacteria concentration and excrete labile DOM rich in N and P	(i) bacterial mineralization of nutrients (ii) micrograzers respond to variable bacteria concentration and excrete labile DOM rich in N and P (iii) bacteria compete for inorganic nutrients
Comment	Typical of most lake eutrophication models that do not include bacteria	Used in model studies where bacteria are simulated but stoichiometry is not specifically a constraint on bacterial production	Most likely the closest representation to reality with bacteria biomass variable and inorganic nutrient uptake used to support bacterial growth requirement

BGD
10, 19731–19772, 2013

Table 3. Equations for C, N and P within nutrients, organic matter, bacteria and zooplankton pools. Note that the pools and processes related to phytoplankton are not included here for brevity since they are not different between the three configurations. For the complete balance equations including the effects of phytoplankton readers are referred to Gal et al. (2009).

	NOBAC	BAC-DIM	BAC+DIM
C	$\frac{\partial POC}{\partial t} = +\sum_z M_z + \sum_a M_a - D_{POC} - S_{POC} - G_{Z3}(POC)$	$\frac{\partial POC}{\partial t} = +\sum_z M_z + \sum_a M_a - D_{POC} - S_{POC}$	$\frac{\partial POC}{\partial t} = +\sum_z M_z + \sum_a M_a - D_{POC} - S_{POC}$
	$\frac{\partial DOC}{\partial t} = D_{POC} - U_{DOC} + \sum_a E_A + \sum_z E_{DOC_z} + DSF$	$\frac{\partial DOC}{\partial t} = D_{POC} - U_{DOC} + \sum_a E_A + \sum_z E_{DOC_z} + E_B + DSF$	$\frac{\partial DOC}{\partial t} = D_{POC} - U_{DOC} + \sum_a E_A + \sum_z E_{DOC_z} + E_B + DSF$
	$\frac{\partial Z_3}{\partial t} = G_{Z3}(POC) - E_{DOC} - R_{Z3} - P_{Z1}$	$\frac{\partial B}{\partial t} = U_{DOC}(B) - E_B - R_B - G_{Z3}(B) - S_B$ $\frac{\partial Z_3}{\partial t} = G_{Z3}(B) - E_{DOC} - R_{Z3} - P_{Z1}$	$\frac{\partial B}{\partial t} = U_{DOC}(B) - E_B - R_B - G_{Z3}(B) - S_B$ $\frac{\partial Z_3}{\partial t} = G_{Z3}(B) - E_{DOC} - R_{Z3} - P_{Z1}$
N	$\frac{\partial PON}{\partial t} = +\sum_z M_z + \sum_a M_a - D_{PON} - S_{PON} - G_{Z3}(PON)$	$\frac{\partial PON}{\partial t} = +\sum_z M_z + \sum_a M_a - D_{PON} - S_{PON}$	$\frac{\partial PON}{\partial t} = +\sum_z M_z + \sum_a M_a - D_{PON} - S_{PON}$
	$\frac{\partial DON}{\partial t} = D_{PON} - U_{DON} + \sum_a E_A + \sum_z E_{DON_z} + DSF$	$\frac{\partial DON}{\partial t} = D_{PON} - U_{DON}(B) + \sum_a E_A + \sum_z E_{DON_z} + DSF$	$\frac{\partial DON}{\partial t} = D_{PON} - U_{DON}(B) + \sum_a E_A + \sum_z E_{DON_z} + DSF$
	$\frac{\partial ZIN_3}{\partial t} = G_{Z3}(PON) - E_{DON} - P_{Z1}$ $\frac{\partial NH_4}{\partial t} = U_{NH4}(A) + DSF - NIT$ $\frac{\partial NO_3}{\partial t} = U_{DON} - U_{NO_3}(A) + DSF + NIT - DEN$	$\frac{\partial BIN}{\partial t} = U_{DON}(B) - E_{NH4} - G_{Z3}(B) - S_B$ $\frac{\partial ZIN_3}{\partial t} = G_{Z3}(B) - E_{DON} - P_{Z1}$ $\frac{\partial NH_4}{\partial t} = +E_{NH4} - U_{NH4}(A) + DSF - NIT$ $\frac{\partial NO_3}{\partial t} = +E_{NH4} - U_{NO_3}(A) + DSF + NIT - DEN$	$\frac{\partial BIN}{\partial t} = U_{DON}(B) + U_{NH_4}(B) + U_{NO_3}(B) - E_{NH4} - G_{Z3}(B) - S_B$ $\frac{\partial ZIN_3}{\partial t} = G_{Z3}(B) - E_{DON} - P_{Z1}$ $\frac{\partial NH_4}{\partial t} = +E_{NH4} - U_{NH4}(A,B) + DSF - NIT$ $\frac{\partial NO_3}{\partial t} = +E_{NH4} - U_{NO_3}(A,B) + DSF + NIT - DEN$
P	$\frac{\partial POP}{\partial t} = +\sum_z M_z + \sum_a M_a - D_{POP} - S_{POP} - G_{Z3}(POP)$	$\frac{\partial POP}{\partial t} = +\sum_z M_z + \sum_a M_a - D_{POP} - S_{POP}$	$\frac{\partial POP}{\partial t} = +\sum_z M_z + \sum_a M_a - D_{POP} - S_{POP}$
	$\frac{\partial DOP}{\partial t} = D_{POP} - U_{DOP} + \sum_a E_A + \sum_z E_{DOP_z} + DSF$	$\frac{\partial DOP}{\partial t} = D_{POP} - U_{DOP}(B) + \sum_a E_A + \sum_z E_{DOP_z} + DSF$	$\frac{\partial DOP}{\partial t} = D_{POP} - U_{DOP}(B) + \sum_a E_A + \sum_z E_{DOP_z} + DSF$
	$\frac{\partial ZIP_3}{\partial t} = G_{Z3}(POP) - E_{DOP} - P_{Z1}$ $\frac{\partial PO_4}{\partial t} = U_{DOP} + DSF - U_{PO4}(A)$	$\frac{\partial BIP}{\partial t} = U_{DOP}(B) - E_{PO4} - G_{Z3}(B) - S_B$ $\frac{\partial ZIP_3}{\partial t} = G_{Z3}(B) - E_{DOP} - P_{Z1} - S_{Z3}$ $\frac{\partial PO_4}{\partial t} = +E_{PO4} - U_{PO4}(A) + DSF$	$\frac{\partial BIP}{\partial t} = U_{DOP}(B) + U_{PO4}(B) - E_{PO4} - G_{Z3}(B) - S_B$ $\frac{\partial ZIP_3}{\partial t} = G_{Z3}(B) - E_{DOP} - P_{Z1} - S_{Z3}$ $\frac{\partial PO_4}{\partial t} = +E_{PO4} - U_{PO4}(A,B) + DSF$

D is particulate decomposition, S is sedimentation (S_{POM} is particulate organic matter sedimentation, S_B is bacterial sedimentation), G_{Z3} is grazing by microzooplankton, M_z is zooplankton mortality and messy feeding, M_a is mortality of phytoplankton R_B is bacterial respiration, R_{Z3} is respiration of microzooplankton P_{Z1} is predation by Z_1, E_A is phytoplankton excretion of DOM, E_{PO4} & E_{NH4} refer to bacterial mineralization of nutrients E_{DOM} is DOM excretion from zooplankton DSF is dissolved sediment flux, NIT is nitrification, DEN is denitrification, U_{DOM} is dissolved organic matter uptake, either independent or linked to B biomass in the case of NOBAC and the other simulations, respectively. U_{NH4}, U_{NO3} and U_{PO4} refer to inorganic nutrient uptake, and the functions are designed to account for phytoplankton uptake only in the case of NOBAC and BAC-DIM, $U(A)$, and phytoplankton and bacteria in the case of BAC+DIM, $U(A,B)$.

BGD
10, 19731–19772, 2013

Table 4. Microbial loop related parameters used in the three model simulations (refer to Gal et al., 2009, for other parameter values).

Parameter	Units	Description	NOBAC	BAC-DIM	BAC+DIM	Comments/Other Literature/Justification
POM parameters						
μ_{POCmax}	d^{-1}	Breakdown rate of POC→DOC	0.07	0.07	0.07	Gal et al. (2009) values adopted. 0.001[(1)]
μ_{PONmax}	d^{-1}	Breakdown rate of PON→DON	0.01	0.01	0.01	0.02[(1)] ; 0.01-0.03[(2)]
μ_{POPmax}	d^{-1}	Breakdown rate of POP→DOP	0.1	0.1	0.1	0.01[(1)] ; 0.01–0.1[(2)]
d_{POM}	m	Diameter of POM particles	5.50×10^{-6}	5.50×10^{-6}	5.50×10^{-6}	Gal et al. (2009) values adopted; 1.50×10^{-5}[(1)]
ρ_{POM}	kg m^{-3}	Density of POM particles	1040	1040	1040	Gal et al. (2009) values adopted; 1.08×10^{3}[(1)]
DOM parameters						
μ_{DOCmax}	d^{-1}	Max mineralisation of DOC→DIC	0.0008	N/A	N/A	Estimated from average output from BAC+DIM
μ_{DOPmax}	d^{-1}	Max mineralisation of DOP→PO_4	0.1	N/A	N/A	0.01[(1)] ; 0.01–0.1[(2)]
μ_{DONmax}	d^{-1}	Max mineralisation of DON→NH_4	0.008	N/A	N/A	calibrated values adopted; 0.02[(1)]; 0.01–0.03[(2)]
Bacteria parameters						
ϑ_B		Arrhenius temperature scaling factor	1.08	1.08	1.08	Gal et al. (2009) values adopted.
T_{STDB}	°C	Standard temperature	20	20	20	Gal et al. (2009) values adopted.
T_{OPTB}	°C	Optimum temperature	30	30	30	Gal et al. (2009) values adopted.
T_{MAXB}	°C	Maximum temperature	38	38	38	Gal et al. (2009) values adopted.
K_{DOB}	mg O_2 L^{-1}	Half saturation constant for dependence of POM/DOM decomposition on DO	1.5	1.5	1.5	Gal et al. (2009) values adopted.
f_{AnB}	–	Reduction factor for anaerobic metabolism	0.8	0.8	0.8	Gal et al. (2009) values adopted.
k_{Br}	d^{-1}	Bacterial respiration rate at 20 °C	N	0.12	0.12	Gal et al. (2009) values adopted.
μ_{DECDOM}	d^{-1}	Maximum bacterial DOC uptake rate	N	0.05	0.05	Gal et al. (2009) values adopted.
K_B	mg C L^{-1}	Half saturation constant for bacteria function	N	0.01	0.01	Gal et al. (2009) values adopted.
K_{BIN}	mg N (mg C)$^{-1}$	Internal C:N ratio of bacteria	N	0.13	0.13	Gal et al. (2009) values adopted.
K_{BIP}	mg P (mg C)$^{-1}$	Internal C:P ratio of bacteria	N	0.0575	0.0575	Gal et al. (2009) values adopted.
K_{Be}	–	DOC excretion	N	0.7	0.7	Gal et al. (2009) values adopted.
μ_{DIMupt}		DIM uptake	N	N	Y	
Micrograzer (Z_3) parameters						
K_{ZIN}	mg N (mg C)$^{-1}$	Internal C:N ratio of micrograzers	0.2	0.2	0.2	0.2[(1)]; 0.24–0.27[(3)]
K_{ZIP}	mg P (mg C)$^{-1}$	Internal C:P ratio of micrograzers	0.016	0.016	0.016	0.01[(1)]; 0.016–0.43[(3)]
P_{zp}	–	Preference of zooplankton for POC	1	0	0	P_{zp} = 1 in NOBAC as no bacteria present; 1[(1)]; 0.75[(4)]
P_{zb}	–	Preference of zooplankton for bacteria	0	1	1	Z_3 assumed to only graze on bacteria
g_{MAX}	mg C L^{-1}(mg Z L^{-1})$^{-1}$$d^{-1}$	Grazing rate	9	9	9	Gal et al. (2009) values adopted;
K_{mf}	–	Messy feeding (grazing efficiency)	0.75	0.75	0.75	Gal et al. (2009) values adopted; 1[(1)]
K_{Ze}	d^{-1}	Excretion fraction of grazing	0.25	0.25	0.25	Gal et al. (2009) values adopted; 0.2[(1)]
K_Z	mg C L^{-1}	Half saturation constant for grazing	0.4	1.5	1.5	0.5[(1)(5)] ; 0.1[(5)] ; 1.64[(6)]
T_{STDZ}	°C	Standard temperature	20	20	20	Gal et al. (2009) values adopted.
T_{OPTZ}	°C	Optimum temperature	24	24	24	Gal et al. (2009) values adopted.
T_{MAXZ}	°C	Maximum temperature	30	30	30	Gal et al. (2009) values adopted.

(1) Bruce et al. (2006); (2) Jorgensen and Bendoricchio (2001); (3) Martin et al. (2005); (4) Gophen and Azoulay (2002); (5) Makler-Pick et al. (2011b); (6) Stemberger and Gilbert (1985)

BGD
10, 19731–19772, 2013

Table 5. Statistical analysis of water quality variables comparing the three microbial loop configurations by ANOVA and multiple comparisons.

Dependent variable	(I) Group	(J) Group	Mean difference (I – J)	Std. error	*P* value (pairwise)	*P* value (between groups)
T	NOBAC	BAC-DIM	−0.135	1.051	0.898	0.989
	NOBAC	BAC+DIM	−0.140	1.051	0.894	
	BAC-DIM	BAC+DIM	−0.005	1.051	0.996	
DO	NOBAC	BAC-DIM	0.052	0.236	0.826	0.237
	NOBAC	BAC+DIM	0.372	0.236	0.117	
	BAC-DIM	BAC+DIM	0.320	0.236	0.178	
NH_4	NOBAC	BAC-DIM	0.048*	0.006	0.000	**0.000**
	NOBAC	BAC+DIM	0.023*	0.006	0.000	
	BAC-DIM	BAC+DIM	−0.025*	0.006	0.000	
NO_3	NOBAC	BAC-DIM	0.015*	0.005	0.002	**0.003**
	NOBAC	BAC+DIM	0.001	0.005	0.794	
	BAC-DIM	BAC+DIM	−0.014*	0.005	0.005	
PO_4	NOBAC	BAC-DIM	−0.000*	0.000	0.000	**0.000**
	NOBAC	BAC+DIM	0.000	0.000	0.958	
	BAC-DIM	BAC+DIM	0.000*	0.000	0.000	
TN	NOBAC	BAC-DIM	−0.072*	0.015	0.000	**0.000**
	NOBAC	BAC+DIM	0.141*	0.015	0.000	
	BAC-DIM	BAC+DIM	0.213*	0.015	0.000	
TP	NOBAC	BAC-DIM	−0.006*	0.001	0.000	**0.000**
	NOBAC	BAC+DIM	−0.008*	0.001	0.000	
	BAC-DIM	BAC+DIM	−0.003*	0.001	0.005	
Nanophytoplankton (A_4)	NOBAC	BAC-DIM	−0.004	0.007	0.555	0.126
	NOBAC	BAC+DIM	−0.013*	0.007	0.048	
	BAC-DIM	BAC+DIM	−0.009	0.007	0.163	
Microcystis (A_2)	NOBAC	BAC-DIM	0.004	0.009	0.669	0.100
	NOBAC	BAC+DIM	−0.014	0.009	0.107	
	BAC-DIM	BAC+DIM	−0.018*	0.009	0.042	
Peridinium (A_1)	NOBAC	BAC-DIM	0.321*	0.057	0.000	**0.000**
	NOBAC	BAC+DIM	0.161*	0.057	0.005	
	BAC-DIM	BAC+DIM	−0.161*	0.057	0.005	
Aulacoseria (A_5)	NOBAC	BAC-DIM	0.033	0.020	0.105	0.125
	NOBAC	BAC+DIM	−0.005	0.020	0.795	
	BAC-DIM	BAC+DIM	−0.0385	0.020	0.060	
Aphanizomenon (A_3)	NOBAC	BAC-DIM	−0.028*	0.005	0.000	**0.000**
	NOBAC	BAC+DIM	−0.012*	0.005	0.009	
	BAC-DIM	BAC+DIM	0.0156*	0.005	0.001	
Predators (Z_1)	NOBAC	BAC-DIM	0.345*	0.168	0.041	**0.001**
	NOBAC	BAC+DIM	0.617*	0.168	0.000	
	BAC-DIM	BAC+DIM	0.272	0.168	0.107	
Macrograzers (Z_2)	NOBAC	BAC-DIM	0.585*	0.171	0.001	**0.001**
	NOBAC	BAC+DIM	0.552*	0.171	0.001	
	BAC-DIM	BAC+DIM	−0.033	0.171	0.848	
Microzooplankton (Z_3)	NOBAC	BAC-DIM	0.241*	0.068	0.000	**0.001**
	NOBAC	BAC+DIM	0.027	0.068	0.691	
	BAC-DIM	BAC+DIM	−0.214*	0.068	0.002	

* The mean difference is significant at the 0.05 level.

BGD
10, 19731–19772, 2013

Table 6. Summary of average values (1997–2001) for C, N, and P contents (mg L^{-1}) and N : P molar ratios of the various food web components in different microbial loop configurations.

Configurations:	NOBAC				BAC-DIM				BAC+DIM			
Variables	C	N	P	N : P	C	N	P	N : P	C	N	P	N : P
DIM	24.63	0.176	0.0036	109 : 1	24.61	0.068	0.0064	23 : 1	25.00	0.157	0.0052	67 : 1
DOM	9.56	0.319	0.0023	307 : 1	7.81	0.421	3.3×10^{-5}	28 475 : 1	1.79	0.050	3.1×10^{-5}	3543 : 1
POM	0.09	0.028	0.0011	57 : 1	0.17	0.137	0.0035	86 : 1	0.26	0.214	0.0040	119 : 1
BAC (B)	N/A	N/A	N/A	N/A	0.06	0.007	0.0032	5 : 1	0.16	0.021	0.0091	5 : 1
Microcystis (A_2)	0.02	0.004	0.0009	9 : 1	0.02	0.002	0.0010	4 : 1	0.03	0.004	0.0011	8 : 1
Peridinium (A_1)	0.19	0.038	0.0006	150 : 1	0.04	0.005	0.0002	59 : 1	0.11	0.018	0.0004	107 : 1
Aphanizomenon (A_3)	2×10^{-3}	3.5×10^{-4}	0.0002	3 : 1	0.02	0.004	0.0018	4 : 1	0.01	0.002	0.0008	4 : 1
Nanophytoplankton (A_4)	0.07	0.022	0.0009	55 : 1	0.08	0.013	0.0016	18 : 1	0.08	0.021	0.0010	47 : 1
Aulacoseria (A_5)	0.06	0.004	0.0006	15 : 1	0.03	0.002	0.0004	10 : 1	0.08	0.005	0.0006	16 : 1
Predators (Z_1)	0.03	0.004	0.0004	27 : 1	0.02	0.003	0.0002	27 : 1	0.01	0.002	0.0001	27 : 1
Macrograzers (Z_2)	0.06	0.012	0.0013	20 : 1	0.03	0.008	0.0008	20 : 1	0.04	0.008	0.0009	20 : 1
Microzooplankton (Z_3)	0.01	0.002	0.0001	28 : 1	2×10^{-3}	4×10^{-4}	3×10^{-5}	28 : 1	0.01	0.001	0.0001	28 : 1
Total dissolved	34.20	0.496	0.0059	186 : 1	32.43	0.489	0.0064	168 : 1	26.79	0.207	0.0052	88 : 1
Total particulate	0.53	0.115	0.0061	42 : 1	0.46	0.180	0.0126	31 : 1	0.79	0.295	0.0182	36 : 1

BGD
10, 19731–19772, 2013

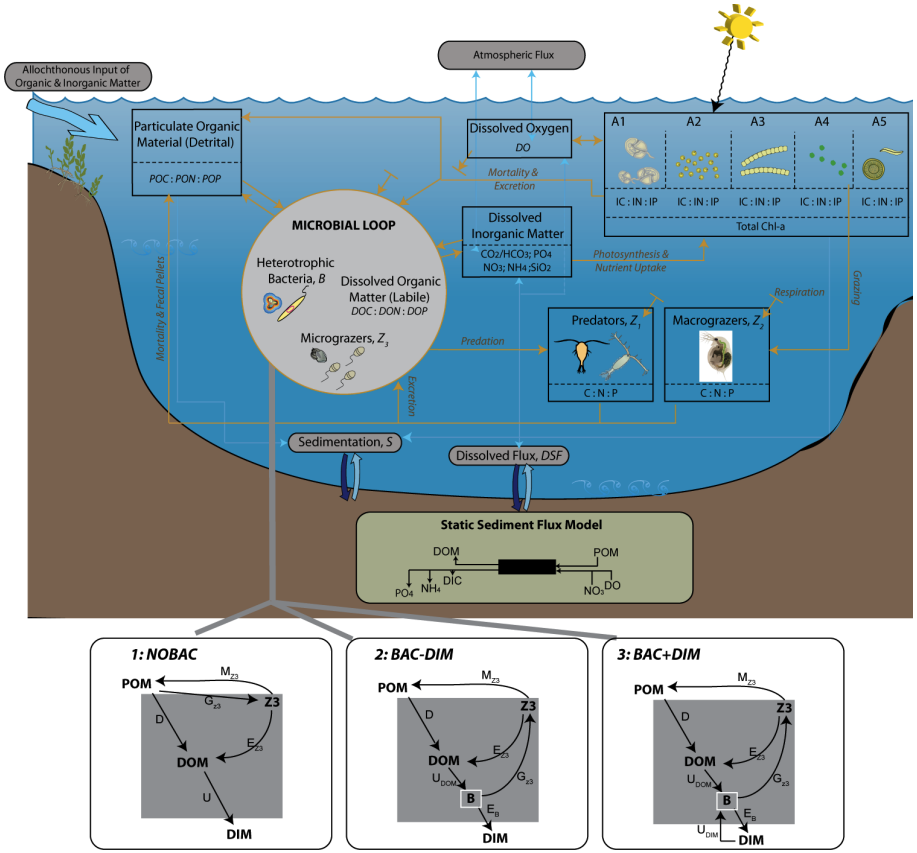

Fig. 1. Conceptual diagram highlighting the general ecosystem model (CAEDYM) configuration for Lake Kinneret (top) and processes and feedbacks for the three microbial loop models (bottom) explored in this study: (1) NOBAC, (2) BAC-DIM, and (3) BAC+DIM (refer to Tables 1 and 3 for notation).

BGD
10, 19731–19772, 2013

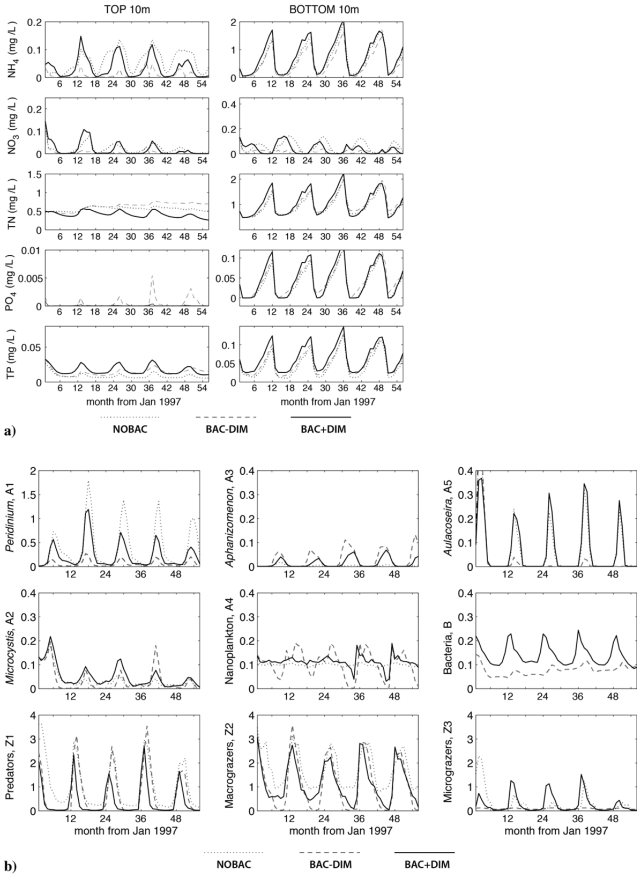

Fig. 2. Comparison of model simulations for **(a)** nutrient variables in the surface 10 m (left) and bottom 10 m (right) of the water column, and **(b)** for the nine simulated biotic groups (mg C L^{-1} for A_{1-5} and B, and mg C m^{-2} for Z_{1-3}).

BGD
10, 19731–19772, 2013

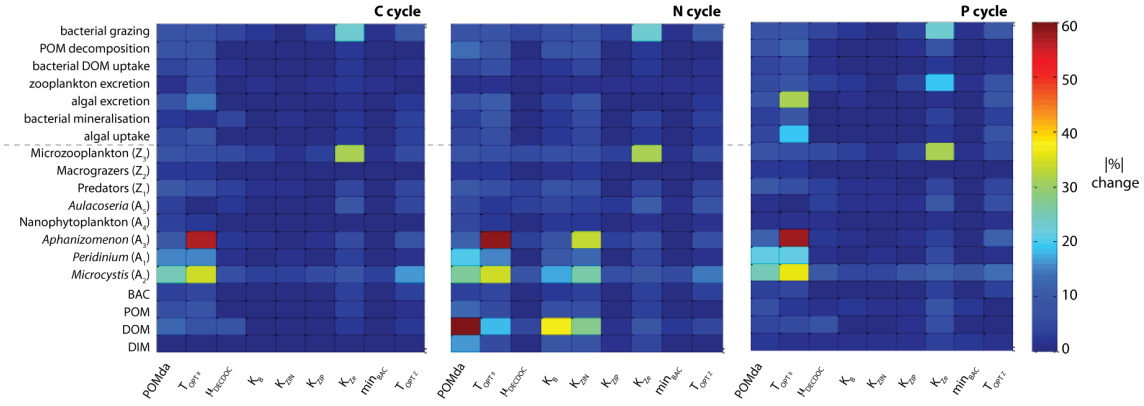

Fig. 3. Local sensitivity analysis of simulated state variables and process rates for the C, N and P cycles presented as the lake average absolute change after a ±20 % parameter shift.

BGD
10, 19731–19772, 2013

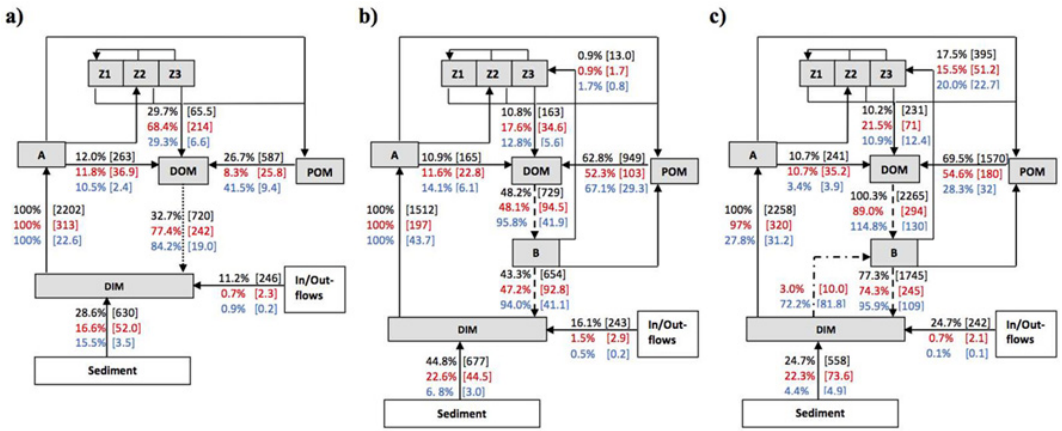

Fig. 4. Summary of simulated annual C (black), N (red) and P (blue) pathways for the three configurations: **(a)** NOBAC, **(b)** BAC-DIM, and **(c)** BAC+DIM. Note the dotted, dashed, and dash-dot lines emphasise configuration specific pathways. Selected fluxes relevant to the analysis are displayed as the lakewide average % relative to the total DIM taken up by phytoplankton and bacteria (where relevant), with the flux rate in brackets ($\times 10^{-5}$ mg L^{-1} d^{-1}).

BGD
10, 19731–19772, 2013

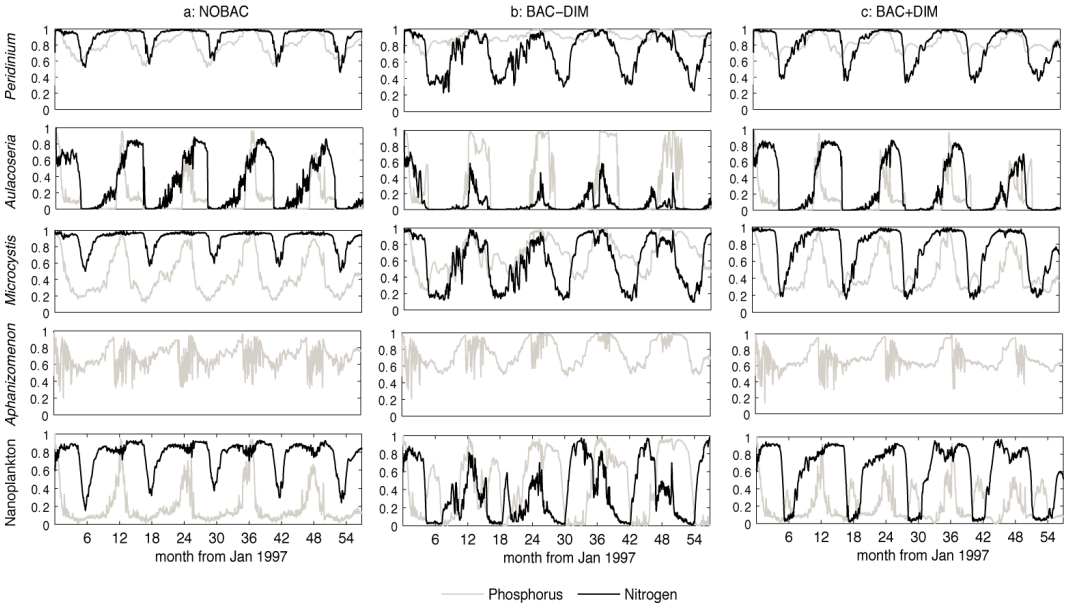

Fig. 5. Comparison of nutrient limitation functions $f_a(N)$ and $f_a(P)$ respectively for the five simulated phytoplankton groups in **(a)** NOBAC, **(b)** BAC-DIM and **(c)** BAC+DIM.

BGD
10, 19731–19772, 2013